Technical Note

Methane gas migration through geomembranes

T. D. Stark[1] and H. Choi[2]

[1]*Professor, Department of Civil and Environmental Engineering, 2217 Newmark Civil Engineering Laboratory, University of Illinois, 205 N. Mathews Ave., Urbana, IL 61801, USA, Telephone: +1 217 333 7394, Telefax: +1 217 333 9464, E-mail: tstark@uiuc.edu*
[2]*Assistant Professor, Department of Civil Engineering, University of Akron, 209D ASEC, Akron, OH 44325-3905, USA, Telephone: +1 330 972 7292, Telefax: +1 330 972 6020, E-mail: hchoi@uakron.edu*

Received 28 April 2004, revised 23 September 2004, accepted 5 October 2004

ABSTRACT: The objectives of this technical note are to review the gas transport mechanisms through flexible geomembranes, and to measure the methane gas transmission rate, permeance, and permeability coefficient of PVC, LLDPE, and HDPE geomembranes by performing the standard gas transport test (ASTM D1434). The measured methane gas permeability coefficient through a PVC geomembrane is 7.55×10^4 ml(STP)·mil/m^2·day·atm, which is slightly less than the gas permeability coefficient of 8.61×10^4 ml(STP)·mil/m^2·day·atm through an LLDPE geomembrane, but slightly higher than the gas permeability coefficient of 3.91×10^4 ml(STP)·mil/m^2·day·atm through an HDPE geomembrane. Thus HDPE exhibits a lower gas permeability coefficient than LLDPE. A field design chart for estimating the methane gas transmission rate for different geomembrane thicknesses is proposed using the measured permeability coefficients for PVC, LLDPE, and HDPE geomembranes and Fick's law. This chart can be used by landfill designers to evaluate the methane gas transmission rate for a selected geomembrane type and thickness and expected methane gas pressure in the landfill.

KEYWORDS: Geosynthetics, Methane gas, Fick's law, Gas transmission ratio, Permeance, Gas permeability coefficient, PVC, linear low-density polyethylene, high-density polyethylene

REFERENCE: Stark, T. D. & Choi, H. (2005). Methane gas migration through geomembranes. *Geosynthetics International*, **12**, No. 2, 000–000

1. INTRODUCTION

To close a waste containment facility, environmental regulations require installation of a final cover system to control infiltration and methane gas release. The final cover system for a lined landfill usually consists, from bottom to top, of: graded landfill surface; a gas-venting layer; a low-permeability hydraulic barrier; a geomembrane; a drainage layer consisting of soil and/or a geosynthetic drainage product; 0.75 m of compacted soil; and 0.15 m of topsoil for growing vegetation.

The main design issues for the geomembrane include differential settlement, wrinkle management, punctures, gas migration, low-temperature behavior for landfills subjected to sub-freezing temperatures, and susceptibility to rats and rodents. This paper focuses on methane gas migration through geomembranes such as PVC, HDPE, and LLDPE.

Several researchers (Haxo *et al.* 1984; Haxo 1990; Haxo and Pierson 1991; Pierson and Barroso 2002) report the permeability of flexible geomembranes to various gases. Haxo *et al.* (1984) show that the gas permeability of polymeric materials differs for a given generic polymer type and structure. In general, the greater the polymer crystallinity, the lower the gas permeability. They also show that the permeability varies with type of gas and temperature. Mark and Gaylord (1964) show that the gas permeability coefficient is independent of geomembrane thickness, assuming no pinholes in the geomembrane, because the gas permeability coefficient is a material property for non-porous media that reflects the permeability of the geomembrane compound.

2. GAS TRANSPORT MECHANISMS

The transport of relatively small gas molecules through a geomembrane is attributed to three different processes:

1. diffusive flow of gas molecules through the non-porous geomembrane;

Article number = 316

2. convective flow through pores or small channels such as cracks, flaws, or pinholes in the geomembrane; and
3. concurrent operation that combines the above mechanisms (Frisch 1956; Mark and Gaylord 1964; Mulder 1991).

Figure 1 compares diffusive flow through a non-porous membrane and convective flow through a porous membrane. The main difference between the two mechanisms is the methane flow path. In the following section, the two mechanisms of gas transport through a geomembrane are described and compared.

2.1. Transport through non-porous media

Geomembranes are considered a non-porous medium if they are free from defects. Although geomembranes are non-porous, gases and vapors can diffuse through a geomembrane by molecular diffusion (Haxo 1990).

The transport of a gas or vapor through a dense, homogeneous, and non-porous geomembrane can be approximated by a solution–diffusion mechanism. In this process, the transport of a permeant occurs in three steps. First, the permeant dissolves and equilibrates in the geomembrane surface. Second, the permeant diffuses in the direction of the lower chemical potential through the geomembrane. Finally, the permeant evaporates from the other surface of the geomembrane into the ambient medium (Mark and Gaylord 1964; Pierson and Barroso 2002). If the boundary conditions on both sides of the geomembrane are maintained constant, a steady-state flux of a permeant can be expressed by Fick's first law as follows:

$$J_D = -D\frac{dc}{dx} \tag{1}$$

where J_D is the diffusive mass flux (g/cm^2-s); D is the diffusion coefficient (cm^2/s); c is the permeant concentration (g/cm^3); and x is the distance through the geomembrane, measured perpendicular to the surface (cm). Therefore the mass flux is proportional to the concentration gradient, dc/dx, through the geomembrane.

Because the concentration of the permeating gas within a geomembrane cannot be measured, and the external pressure of the gas is routinely measured on both the surfaces of the geomembrane during a gas transport test, the external gas pressure can be used to express the gas concentration within the geomembrane. The solubility of a gas in a geomembrane can be described by Henry's law, which indicates a linear relationship between the external pressure and the gas concentration inside the geomembrane. Therefore the gas concentration can be expressed as

$$c = S \times p \tag{2}$$

where S is Henry's law constant or solubility coefficient, and p is the external pressure outside the geomembrane. The solubility coefficient is a thermodynamic parameter that describes the amount of permeant sorbed by a geomembrane. The solubility coefficient of gases in polymers is extremely low, and the diffusion coefficient of gases is considered constant. In this ideal case, Fick's first law is applicable. On the other hand, the solubility coefficient of organic liquids is relatively high, and the diffusion coefficient becomes dependent on the concentration of the liquid. For example, the diffusion coefficient increases with increasing concentration of the liquid (Mulder 1991). In this situation, Fick's first law is not applicable.

Considering here the transport of gas through a geomembrane, by substituting Equation 2 into Equation 1 and integrating across the geomembrane along with applying boundary conditions of the external pressure p_{in} on the feed side ($x = 0$) and p_{out} on the permeate side ($x = t$) where t is the thickness of the geomembrane, the gas mass flux through the geomembrane can be expressed as

$$J_D = P_D\frac{(p_{in} - p_{out})}{t} \tag{3}$$

where P_D is the diffusive gas permeability coefficient ($= D \times S$), and t is the geomembrane thickness. Equation 3 indicates that the diffusive mass flux of a gas through a geomembrane is proportional to the pressure difference (i.e. $p_{in} - p_{out}$) across the geomembrane, and inversely proportional to geomembrane thickness.

The diffusion coefficient (D) and solubility coefficient (S) of various gases for a geomembrane are dependent on the molecular size of each gas. In general, the diffusion coefficient increases with decreasing molecular size. In contrast, the solubility coefficient of a gas increases with increasing molecular size of the gas. These two opposite trends usually cancel each other when evaluating the diffusive gas permeability of a geomembrane. However, this fact does indicate that smaller gas molecules do not necessarily exhibit a higher permeability than larger gas molecules.

Because the diffusion coefficient and solubility coefficient are generally dependent on temperature, the diffusive gas permeability coefficient (P_D) is temperature dependent as shown below by the Arrhenius law (Frisch 1956; Mark and Gaylord 1964):

$$P_D = P_{D0}\exp\left(-\frac{E_P}{RT}\right) \tag{4}$$

where P_{D0} is the reference gas permeability at a standard state; E_P is the summation of the activation energy for diffusion and the heat of solution of the gas in the polymer (the sum of the heat of condensation and the heat of mixing); R is the ideal gas constant; and T is absolute

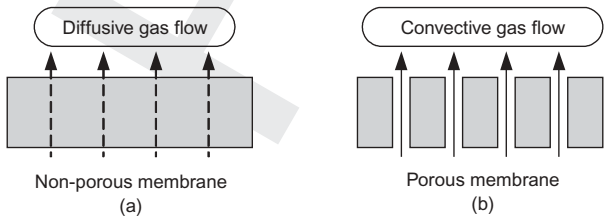

Figure 1. Schematic comparison of gas flow mechanisms: (a) diffusive flow through a non-porous membrane; (b) convective flow through a porous membrane

temperature (K). As shown in Equation 4, the diffusive gas permeability coefficient generally increases with temperature.

2.2. Transport through porous media

Though geomembranes are considered non-porous, they may contain small channels or passages, such as cracks, flaws, or pinholes, in the long-range structure through which convective permeation of small gas molecules may occur. Two different convective flow mechanisms are considered according to the size of the channel in the geomembrane. For a large channel-radius (i.e. $r > 10\ \mu$m) and high gas pressure applied to the geomembrane, viscous flow or Poisseuille flow occurs in which gas molecules collide with each other. For a small channel-radius (i.e. $r < 10\ \mu$m) and low gas pressure applied to the geomembrane, Knudsen flow prevails (Frisch 1956; Mulder 1991). In this paper, viscous flow is considered as the convective gas flow through a geomembrane channel or defect.

The simplest representation of viscous flow is that gas permeates through a number of parallel cylindrical channels across the geomembrane. The length of each cylindrical channel is equal to the geomembrane thickness (t) multiplied by a tortuosity factor (τ). The value of τ is equal to unity if all the cylindrical channels are perpendicular to the geomembrane surface. Otherwise, the value of τ is greater than unity. Assuming all the channels have the same radius, the convective mass flux by viscous flow can be represented by the Hagen-Poisseuille equation as follows:

$$J_C = \frac{nr^2}{8\eta\tau}\frac{(p_{in} - p_{out})}{t} \tag{5}$$

where n is the porosity, i.e. the volume fraction of channels in the geomembrane; r is the channel radius; and η is the viscosity of the gas. The convective mass flux is proportional to the pressure gradient, and thus the convective gas permeability coefficient (P_C) can be expressed as

$$P_C = \frac{nr^2}{8\eta\tau} \tag{6}$$

Equation 6 shows that the convective gas permeability coefficient is a function of the number, size, and shape of channels in the geomembrane, i.e. in terms of the porosity, channel radius, and tortuosity. Because the viscosity of gas is directly proportional to temperature, the convective gas permeability coefficient shows negative temperature dependence (Mark and Gaylord 1964).

2.3. Combination of diffusive and convective transport

A unified gas transport model combining diffusive and convective flow is used to represent the gas migration phenomenon through a geomembrane in which small channels such as cracks, flaws, or pinholes exist. However, it is not easy to combine the two flow mechanisms into a single mathematical expression because the diffusive and convective flow mechanisms are coupled (Frisch 1956). A conceptual and qualitative expression for the total mass flux (J) of a gas through a geomembrane can be written as follows:

$$J = (1 - n)J_D + J_C \tag{7}$$

For the case of a perfectly non-porous geomembrane without any small channels (i.e. porosity is equal to zero), the contribution of convective flux (J_C) (see Equation 5) is omitted from Equation 7, and thus the gas transport occurs by diffusive flow mechanism only.

3. MEASUREMENT OF METHANE GAS PERMEABILITY

3.1. Experimental procedure

To address the methane gas migration through typical geomembranes used for final cover systems, three types of geomembrane, PVC, LLDPE, and HDPE, were tested; they are described in Table 1. The geomembrane thickness measurements in Table 1 were performed in accordance with ASTM D5199 (ASTM 2001), which uses a micrometer to determine geomembrane thickness directly instead of using the material density. Geomembrane density was measured using ASTM D792 (ASTM 2000) and ASTM D1505 (ASTM 2003b).

The methane transmission rates through the PVC, LLDPE, and HDPE geomembranes in Table 1 were measured at a gas pressure gradient of 34.5 kPa and a test temperature of 25°C. All testing was performed at a relative humidity of 100% in accordance with the ASTM D1434 test method (ASTM 2003a) by TRI/Environmental of Austin, Texas. TRI/Environmental employs a permeation instrument to analyze the transmission rate of pure methane gas through a geomembrane specimen. Each test is performed using a split cell with the two halves

Table 1. Material properties of tested geomembranes

Geomembrane	Nominal thickness [mm (mils[a])]	Measured thickness [mm (mils)]	Nominal density (g/cm^3)	Measured density (g/cm^3)	Geomembrane manufacturer
Polyvinyl chloride (PVC)	0.76 (30)	0.72 (28.5)	1.20	1.27	Canadian General Tower, Ontario, Canada
Linear low-density polyethylene (LLDPE)	1.0 (40)	1.07 (42)	0.92	0.93	GSE Lining Technologies, Houston, TX
High-density polyethylene (HDPE)	1.0 (40)	1.12 (44)	0.94	0.95	Agru America, Kingwood, TX

[a]1 mil = 0.001 in.

separated by the test geomembrane. The methane is introduced on the 'challenge' side, and detection of the permeating methane is performed on the 'collection' side (TRI/Environmental 1993, 2000).

High-pressure liquid chromatography (HPLC) water (high-purity water) is placed in the lower half of the challenge side to generate a relative humidity of 100%. The test cell is assembled and clamped with the test material located between the two halves, serving as a barrier to the methane. Methane gas is introduced into the lower half of the challenge side and flushed at a high flow rate, 30 cm^3/min, for 10 min. The flow rate is then reduced to 5 cm^3/min and a methane pressure of 34.5 kPa is established. A pressure gage is attached to the end of the methane stream on the challenge side to monitor and maintain the methane pressure throughout the test.

A flow of 15 cm^3/min of nitrogen gas is established on the upper half of the collection side. The nitrogen moves across the surface of the test geomembrane before going to a flame ionization detector (FID) sensor. Methane permeation is monitored continuously by the FID sensor until 2 days of steady-state permeation is observed. A calibration relationship for the FID is established by injecting pure methane and checking linearity of the sensor by using the injection volume of 5, 7.5, and 10 μl.

3.2. Test results and discussions

The results of the methane gas transport testing are summarized in Table 2. The methane gas transmission rate, permeance, and gas permeability coefficient in Table 2 are calculated using ASTM D1434 (ASTM 2003a) and have metric units. It is assumed that the tested geomembrane specimens do not have any cracks, flaws, or pinholes. Thus all the geomembranes tested in this research are considered non-porous media, and thus the measured gas permeability coefficient is equal to the diffusive permeability coefficient.

Table 2 shows that the methane gas transmission rate for the 0.76 mm thick PVC geomembrane is higher than the methane gas transmission rate for the 1.0 mm thick LLDPE and 1.0 mm thick HDPE geomembranes. This difference is caused primarily by the geomembrane thickness not being considered in the calculation of the methane gas transmission rate, so the thinnest geomembrane exhibits the highest gas transmission rate (Haxo *et al.* 1984). The gas permeability coefficient is a material property and is independent of geomembrane thickness. Table 2 shows that the LLDPE geomembrane exhibits a methane gas permeability coefficient that is higher than that of the PVC geomembrane.

The trend for the LLDPE geomembrane to exhibit a higher methane gas permeability coefficient than the PVC geomembrane is also observed in experimental data presented by Mulder (1991). Figure 2 shows the comparison of the gas permeability coefficient between an LDPE (low-density polyethylene) and PVC geomembrane for various permeating gases. The LDPE geomembrane permeated by methane gas exhibits a gas permeability coefficient that is two orders of magnitude higher than that of the PVC geomembrane. This difference is much greater than the test result in Table 2. It may be supposed that the LDPE has not the same material property with the LLDPE. In Figure 2, the Lennard-Jones diameter represents the size of gas molecules. Methane gas has a Lennard-Jones diameter of 3.82×10^{-4} μm. The other gases used in Figure 2 are hydrogen, oxygen, nitrogen, and carbon dioxide, which have Lennard-Jones diameters of 2.9×10^{-4}, 3.43×10^{-4}, 3.68×10^{-4}, and 4.0×10^{-4} μm respectively.

As previously described, the gas permeability coefficient of a non-porous geomembrane with no cracks, flaws, or pinholes is a material property and not a function of

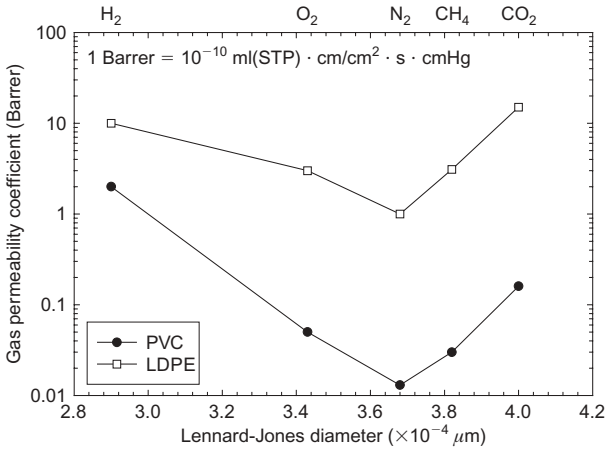

Figure 2. Gas permeability coefficient of various gases through PVC and LDPE geomembranes (from Mulder 1991)

Table 2. TRI/Environmental (1993, 2000) methane gas migration test results (ASTM D1434)

Geomembrane	Replicate test number	Gas transmission rate [ml(STP)/m^2·day]		Permeance [ml(STP)/m^2·day·atm]	Gas permeability coefficient [ml(STP)·mil/m^2·day·atm]
		Measured values	Average values		
0.76 mm PVC	1	879	901	2.65×10^3	7.55×10^4
	2	923			
1.0 mm LLDPE	1	667	687	2.05×10^3	8.61×10^4
	2	706			
1.0 mm HDPE	1	304	302	8.88×10^2	3.91×10^4
	2	300			

All tests performed at a methane gas pressure of 34.5 kPa, 100% relative humidity, and 25°C.

geomembrane thickness. In addition, Mark and Gaylord (1964) show that the gas permeability coefficient of membranes thicker than 0.025 mm generally tends to be independent of thickness, and thus is constant. Haxo and Pierson (1991) also show that each geomembrane has a similar value of the gas permeability coefficient for different thicknesses. Therefore the gas permeability coefficient can be considered as an intrinsic characteristic of the geomembranes.

More importantly, all the values of methane gas permeability coefficient and hydraulic conductivity in Table 2 are extremely low. As a result, significant methane gas migration through any of these geomembranes is not expected in field situations, especially if a gas-venting layer is installed below the geomembrane. If a gas-venting layer is installed below the geomembrane, the methane gas pressure under the geomembrane probably will not reach the pressure used in the testing conducted herein (34.5 kPa). In fact, field evidence of the low transmission rate through PVC is whale backs or bubbles that develop in PVC geomembranes in landfill covers (see Figure 3) and lagoons. Of course, defects/holes in the geomembrane or seams will result in gas migration, so careful CQA and CQC procedures should be followed for landfill covers to ensure containment of the methane gas. The leakage from defects can far exceed the leakage, if any, through an intact geomembrane.

4. FIELD DESIGN CONSIDERATIONS

Assuming a geomembrane is free from any small channels, the measured gas permeability coefficients of the PVC, LLDPE, and HDPE geomembranes in Table 2 can be used to obtain a relationship between the methane gas transmission rate and geomembrane thickness for a given temperature and pressure using Equation 3. This relationship is plotted in Figure 4 for two values of methane gas pressure, i.e. 10.0 kPa and 34.5 kPa, at a temperature of 25°C. The temperature of 25°C is close to the seasonal average temperature in a typical landfill. The methane gas transmission rate for a selected geomembrane and its thickness and methane gas pressure expected in the landfill can be interpolated from Figure 4. Figure 4 shows that PVC exhibits a methane transmission rate higher than HDPE, but less than LLDPE for the given range of geomembrane thickness. In addition, the difference between PVC and LLDPE increases as the methane gas pressure increases.

Figure 3. Inflation of PVC geomembrane by methane gas in landfill cover

5. CONCLUSIONS

The following conclusions are based on the data and interpretation presented herein.

1. The TRI/Environmental (1993, 2000) test results presented herein suggest that the methane gas permeability through a PVC geomembrane is less than that through an LLDPE geomembrane, but slightly higher than that through a HDPE geomembrane. The test was performed at a gas pressure gradient of 34.5 kPa and a test temperature of 25°C.
2. By assuming that the geomembranes specimens tested herein are free from any small migration channels such as cracks, flaws, or pinholes, a field design chart is presented. The field design chart is developed using the measured gas permeability coefficients for the PVC, LLDPE, and HDPE geomembranes for a temperature of 25°C and Fick's law. By interpolating the trend lines for two typical methane gas pressures (10.0 kPa and 34.5 kPa), this chart can be used to evaluate the methane gas transmission rate for a selected geomembrane type and thickness and the methane gas pressure expected below the landfill cover system. The design chart shows that PVC exhibits a methane transmission rate higher than HDPE, but less than LLDPE for the given range of geomembrane thickness. In addition, the difference between PVC and LLDPE increases as the methane gas pressure increases.
3. The gas permeability coefficients shown in Table 2 are sufficiently low to ensure that little, if any, methane migration will occur through a PVC,

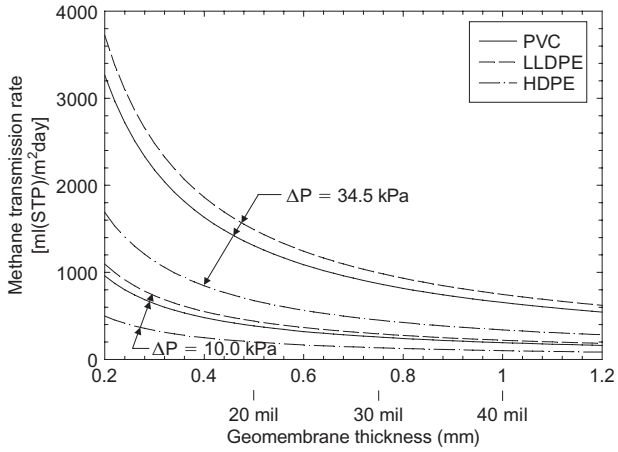

Figure 4. Design chart for methane gas transmission rate of PVC, LLDPE, HDPE geomembranes at a temperature of 25°C

LLDPE, or HDPE geomembrane. This is especially true if a gas-venting layer is installed below the geomembrane.

NOTATIONS

Basic SI units are given in parentheses.

- c permeant concentration (kg/cm^3)
- D diffusion coefficient (m^2/s)
- E_P activation energy for permeation (J)
- J total mass flux ($kg/m^2 \cdot s$)
- J_C convective mass flux ($kg/m^2 \cdot s$)
- J_D diffusive mass flux ($kg/m^2 \cdot s$)
- n porosity (dimensionless)
- P_C convective gas permeability coefficient (m^2/s)
- P_D diffusive gas permeability coefficient (m^2/s)
- P_{D0} reference gas permeability coefficient at a standard state (m^2/s)
- p_{in} external pressure on the feed side (Pa)
- p_{out} external pressure on the permeate side (Pa)
- R ideal gas constant, 8.3143 ($m^3Pa/mol \cdot K°$)
- r channel radius (m)
- S Henry's law constant or solubility constant (dimensionless)
- T absolute temperature (K)
- t geomembrane thickness (m)
- x distance (m)
- η gas viscosity (Pa·s)
- τ tortuosity factor (dimensionless)

ABBREVIATIONS

- HDPE high-density polyethylene
- LDPE low-density polyethylene
- LLDPE linear low-density polyethylene
- PVC polyvinyl chloride
- STP Standard temperature and pressure, denoting an exact reference temperature of 0°C (273.15 K) and pressure of 1 atm (defined as 101.325 kPa)

REFERENCES

ASTM (2000). Standard Test Methods for Density and Specific Gravity (Relative Density) of Plastics by Displacement, D792. West Conshohocken, PA: American Society for Testing and Materials.

ASTM (2001). Standard Test Methods for Measuring the Nominal Thickness of Geosynthetics, D5199, West Conshohocken, PA: American Society for Testing and Materials.

ASTM (2003a). Standard Test Method for Determining Gas Permeability Characteristics of Plastic Film and Sheeting, D1434. West Conshohocken, PA: American Society for Testing and Materials.

ASTM (2003b). Standard Test Method for Density of Plastics by the Density-Gradient Technique, D1505. West Conshohocken, PA: American Society for Testing and Materials.

Frisch, H. L. (1956). Gas permeation through membrane due to simultaneous diffusion and convection. Journal of Physical Chemistry, **60**, 1177–1181.

Haxo, H. E. (1990). Determining the transport through geomembranes of various permeants in different applications. In Geosynthetic Testing for Waste Containment Applications (ed. R. M. Koerner), STP 1081, pp. 75–94. West Conshohocken, PA: American Society for Testing and Materials.

Haxo, H. E. & Pierson, P. (1991). Permeability testing. In Geomembranes Identification and Performance Testing (eds A. Rolling and J-M. Rigo), RILEM Report 4, pp. 219–240. RILEM.

Haxo, H. E., Miedema, J. A. & Nelson, N. A. (1984). Permeability of polymeric membrane lining materials. Proceedings of the International Conference on Geomembrane, Denver, CO, pp. 151–156.

Koerner, R. M. (1998). Designing with Geosynthetics, 4th edn. Prentice Hall.

Mark, H. F. & Gaylord, N. G. (1964). Encyclopedia of Polymer and Technology: Plastics, Resins, Rubbers, Fibers. New York: Interscience Publishers.

Mulder, M. (1991). Basic Principles of Membrane Technology. Kluwer Academic Publishers.

Pierson, P. & Barroso, M. (2002). A pouch test for characterizing gas permeability of geomembranes. Geosynthetics International, **9**, No. 4, 345–372.

Thomas, R. W., Stark, T. D. & Choi, H. (2003). Air channel testing of thermally bonded PVC geomembrane seams. Geosynthetics International, **10**, No. 2, 56–69.

TRI/Environmental, Inc. (2000). Methane Permeation Testing, Letter Report No. E2138-37-03. Austin, TX: TRI/Environmental, Inc., 3 pp.

TRI/Environmental, Inc. (1993). Permeability of 60 mil HDPE Geomembrane to Methane Gas, Letter Report. Austin, TX: TRI/Environmental, Inc., 3 pp.

The Editors welcome discussion in all papers published in Geosynthetics International. Please email your contribution to discussion@geosynthetics-international.com by ???.